A 24-channel shim array for real-time shimming of the human spinal cord: Characterization and proof-of-concept experiment

Ryan Topfer[1], Kai-Ming Lo[2], Karl Metzemaekers[2], Donald Jette[2], Hoby P. Hetherington[3], Piotr Starewicz[2], and Julien Cohen-Adad[1,4]

[1]Institute of Biomedical Engineering, Ecole Polytechnique de Montréal, Montreal, QC, Canada, [2]Resonance Research Inc., Billerica, MA, United States, [3]Department of Radiology, University of Pittsburgh, Pittsburgh, PA, United States, [4]Functional Neuroimaging Unit, CRIUGM, Université de Montréal, Montreal, QC, Canada

Target Audience: MR scientists and clinicians interested in spectroscopic or echo planar imaging of the spinal cord.

Introduction: Spatial variation in magnetic susceptibility within the magnetizing b_0 field of the scanner gives rise to a spatially varying secondary field b_χ, leading to spin dephasing and its corollaries: signal dropout and geometric distortion in T2*-weighted imaging, and line-broadening in MR spectroscopy. Though auxiliary shim fields are commonly adjusted at the outset of a scan to correct for susceptibility effects, adjustments typically ignore the dynamic effects of respiration[1]. However effective at clinical field strengths when imaging regions away from air-tissue interfaces, static shimming cannot adequately compensate for the large, fluctuating field inhomogeneity near the lungs, making imaging of the spinal cord problematic, particularly at high field. This study describes initial calibration and proof-of-concept phantom experiments using a novel 24-channel shim system, designed for real-time shimming in MR studies of the human spinal cord.

Theory: From Biot-Savart it is known that passing a steady current through a uniform conductor results in a magnetic induction field b_c which is (1) linear with the applied current, and (2) harmonic except at the conductor boundaries. For a given coil element (index c) the resulting field can be considered a scaling of the applied current i_c by a term depending on the coil position and geometry $b_c(\boldsymbol{r}) = i_c a_c(\boldsymbol{r})$. Considering a network of N_c coils, the total longitudinal field at position $\boldsymbol{r}$ can be expressed as $b_z(\boldsymbol{r}) = (b_0 + b_\chi(\boldsymbol{r}) + \sum_{c=1}^{N_c=24} i_c a_c(\boldsymbol{r}))\,\hat{z}$. In vector form, the ideal shim currents, under which $b_z(\boldsymbol{r}) \rightarrow b_0$, should therefore satisfy $A\mathbf{i_c} = -\mathbf{b_\chi}$, where $\mathbf{i_c}$ is the $[N_c \times 1]$ column vector of coil currents and A is the matrix operator (1 row per image voxel) formed by placing the set of scaling parameters $\mathbf{a_c}$ along its columns.

Methods: *I. Shim system and RF coil*: The shim array (Fig. 1) consists of 24 rectangular planar electrical coils. The coils were fabricated using a double-sided flex circuit and each coil (140×70 mm^2) features 10 turns. Cooling layers lie above and below the coils. The shim structure, with cover and thin cushion atop it, lies within the MRI patient table, in close proximity to the subject's spine. The transceiver phased array consists of eight (80×90 mm^2) flat rectangular surface coils arranged in 2 columns along the spine axis for a total coverage of 19×35 cm^2. To avoid interaction with the shim coil, the array was shielded 3 cm away from the loops. Adjacent coils were decoupled inductively using transformer decoupling to a level of -18 dB or better.

II. Calibration experiment: Empirical estimation of $\mathbf{a_c}$ parameters via GRE field mapping[2]. *Protocol*: A rectangular plastic container nearly filled with water was used as a phantom (dimensions: 34×16×44 cm^3). GRE scans were performed at 3.0 T (Siemens Healthcare) with parameters: TE=[4.92, 7.38] ms, TR=300 ms; flip angle 56°; spatial resolution=6.81×6.81 mm^2 in-plane, with 26 coronal slices of thickness 5.0 mm, and 5.5 mm between slices, for an effective FOV=354×143×490 mm^3. Field maps of the phantom were acquired in 2 states per channel: $i_c = [-0.5, +0.5]$ amperes, while current was zeroed in the remaining 23 channels. In addition, a field map was acquired with all channels set to 0 amperes, giving a total of 49 independent scans $(2N_c + 1)$. *Processing*: All 49 phase difference images were unwrapped[3] on a slice-by-slice basis using a rectangular mask (30.0×12.1×36.8 cm^3) to avoid incorporating regions with residual distortion or poor signal. After scaling phase to frequency, to further reduce the effects of noise and distortion, unwrapped phase images were linearly interpolated along $\hat{z}$ to yield an isotropic voxel spacing and then filtered using a normalized spherical kernel[4,5] (radius = 2 voxels), thereby extracting the harmonic phase owing to background susceptibility sources and to the shim itself. With the shared zero-current acquisition, 3 effective frequency (i.e. field) maps were available by which $\mathbf{a_c}$ was estimated through a linear least-squares regression of frequency to current.

III. Phantom experiment: To examine the effect of shimming, four GRE scans were performed on a simple phantom – an air-filled, roughly ellipsoidal, 350 mL plastic shampoo bottle centered within a water-filled plastic box (dimensions: 20×20×30 cm^3). GRE scan parameters were: flip angle 56°; 4.86×4.86 mm^2 resolution in-plane, and 7 coronal slices gapped by 7.5 mm; with all other parameters identical to those of the calibration protocol. The phantom was first scanned with some air squeezed out of the bottle (crudely analogous to an "expired" respiratory state). Phase data were then unwrapped slice-wise and linearly interpolated to the grid spacing of the $\mathbf{a_c}$ calibration images. Interpolated magnitude images were thresholded at 10 % to create binary masks M by which to exclude regions of air from the shim optimization. Optimal shim currents $\mathbf{i_c}$ (determined by minimizing $\left\|\mathrm{M}(A\mathbf{i_c} + \mathbf{b_\chi})\right\|_2^2$ via conjugate gradients) were then applied before reacquiring the field map. This procedure was repeated after refilling the phantom bottle with air (analogous to an "inspired" respiratory state).

Results and Discussion: The expected properties of the shim fields, namely (1) linearity with applied current, and (2) smooth (harmonic) spatial profiles, are demonstrated in Fig. 2. After masking, the two effective shim volumes were each approximately 1.1 L. Using the two sets of optimized currents to shim over the respective volumes reduced the standard deviations of the field 35.5% and 31.3% for the "squeezed" and "unsqueezed" cases respectively. Though shimming resulted in some localized regions of increased inhomogeneity (e.g., on the right in Fig. 3: an increase in the extent of the negative lobes can be seen in the central portion of the FOV – that is, along the sides of the bottle), this can be explained by the nature of the least-squares shim optimization: given that the field of the shims cannot perfectly model that produced by arbitrary susceptibility distributions, the best overall fit will generally improve the homogeneity of the majority of shimmed voxels at the expense of a minority. Future experiments will look to minimizing this effect by reducing the shim volume and shimming in a per-slice fashion.

Acknowledgements: This work was funded by the NSERC, CFI, FRQS.

References: **[1]** Verma, *Magn Reson Med,* 2014 ; **[2]** Van Zijl, *J Magn Reson Ser A*, 1994; **[3]** Jenkinson, *Magn Reson Med*, 2003; **[4]** Li, *J Magn Reson*, 2001; **[5]** Sun, *Magn Reson Med*, 2014.

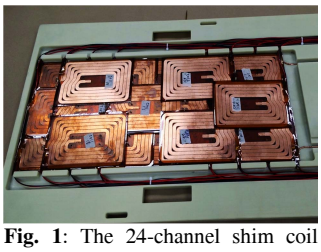

Fig. 1: The 24-channel shim coil array (above) sits, beneath the RF coils, within the patient bed table.

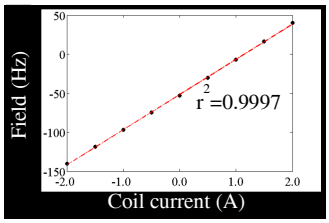

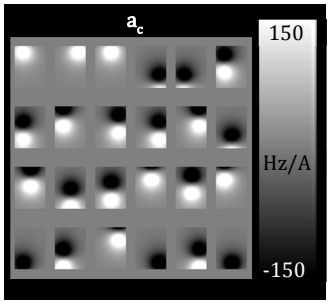

Fig. 2: *Top*: Field linearity with coil-current for channel c=1, testing 9 currents equally spaced between i_c = [-2.0, +2.0] amperes. The field measurements were averaged over a spherical volume (radius = 2 voxels) positioned centrally in the FOV. *Bottom*: Coronal slices of the fitted $\mathbf{a_c}$ parameters for each of the 24 shim coils, used to formulate operator A.

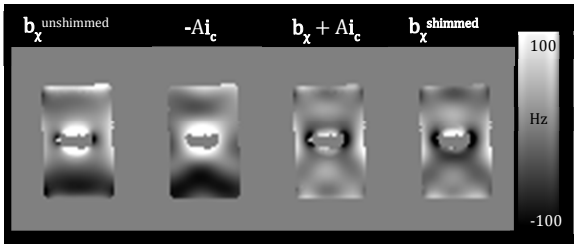

Fig. 3: Shimming the "squeezed" phantom (coronal orientation). The unshimmed field map $\mathbf{b_\chi}$ is modeled as a superposition of fields owing to the shim coils ($-A\mathbf{i_c}$). The predicted residual field inhomogeneity ($\mathbf{b_\chi} + A\mathbf{i_c}$) closely resembles the $\mathbf{b_\chi}$ field map reacquired after shimming.